Improved photocatalysis of perfluorooctanoic acid in water by Ga_2O_3/UV system assisted by peroxymonosulfate

Bentuo Xu[a,b], John L. Zhou[a*], Ali Altaee[a], Mohammad B. Ahmed[a], Md Abu Hasan Johir[a], Jiawei Ren[a], Xiaowei Li[c]

[a] Centre for Green Technology, School of Civil and Environmental Engineering, University of Technology Sydney, 15 Broadway, NSW 2007, Australia

[b] School of Life and Environmental Science, Wenzhou University, Wenzhou 325035, China

[c] School of Environmental and Chemical Engineering, Institute for the Conservation of Cultural Heritage, Shanghai University, Shanghai 200444, China

Corresponding author:
Prof John L. Zhou
Centre for Green Technology
School of Civil and Environmental Engineering
University of Technology Sydney
15 Broadway, NSW 2007
Australia
Email: junliang.zhou@uts.edu.au

Abstract

Perfluorooctanoic acid (PFOA) has attracted considerable attention worldwide due to its widespread occurrence and environmental impacts. This research focused on the photocatalytic process for the treatment of PFOA in water. Gallium oxide (Ga_2O_3) and peroxymonosulfate (PMS) were mixed directly in the PFOA solution and irradiated under different wavelengths of light resources. It showed excellent performance that 100% PFOA was degraded within 90 min and 60 min under 254 nm and 185 nm UV irradiation, respectively. Moreover, the degradation efficacy was unaffected by initial PFOA concentration from 50 ng L^{-1} to 50 mg L^{-1}. Acidic solution (pH 3) improved the degradation process. The quantum yield in the PMS/Ga_2O_3 system under UV light (254 nm) was estimated to be 0.009 mol $Einstein^{-1}$. Scavengers such as *tert*-butanol (*t*-BuOH), disodium ethylenediaminetetraacetate (EDTA-Na_2) and benzoquinone (BQ) were added into PFOA solution to prove that sulfate radicals ($SO_4^{\bullet-}$), superoxide radical ($O_2^{\bullet-}$) and photogenerated electrons (e^-) were the main active species with strong redox ability for PFOA degradation in PMS/Ga_2O_3/UV system. Combined with the intermediates analysis, PFOA was degraded stepwise from long chain compound to shorter chain intermediates. In addition, PFOA in real wastewater exhibited similar degradation efficiency and 75-85% TOC was removal by Ga_2O_3/PMS under 254 nm UV irradiation. Therefore, Ga_2O_3/PMS system was highly effective for PFOA photodegradation under UV irradiation, which has potential to be applied for the perfluoroalkyl substances (PFAS) treatment in water and wastewater.

Keywords: Perfluorooctanoic acid; Photocatalytic pathway; PMS/Ga_2O_3/UV system; Quantum yield; Sulfate radicals

1. Introduction

Perfluoroalkyl substances (PFAS), anthropogenic compounds characterised by their fully fluorinated hydrophobic carbon and a hydrophilic end group, have been applied in many industrial, commercial and domestic products and as the key ingredient in aqueous film-forming foams since the 1950s (Braunig et al., 2019). Due to the highly stable carbon-fluorine bond with a bond energy of 544 kJ mol^{-1} (Saleh et al., 2019), PFAS are ubiquitous in the environment and globally detected in many environmental matrices and even in human tissues (Jian et al., 2018; Mazzoni et al., 2019). For example, the Williamtown site from Sydney, Australia was found to contain up to mg L^{-1} level of perfluorooctanoic acid (PFOA) and perfluorooctane sulfonate (PFOS), two kinds of well-known PFAS, over the past decades (www.health.nsw.gov.au/environment). Both substances worked their way through the surface water or soil to the groundwater underneath the site, leading to the land contamination close to the site (Anderson et al., 2018; Janda et al., 2019). Until now, these chemicals have been reported to be linked to many human diseases such as kidney cancer (Mulabagal et al., 2018), thyroid disease (Blake et al., 2018), testicular cancer (Mastrantonio et al., 2017) and pregnancy-induced hypertension (Apelberg et al., 2007; Holtcamp, 2012). Therefore, as a precautionary approach, new technology with strong degradation ability for PFAS removal is urgently needed to mitigate PFAS contamination.

As the most representative class of PFAS, PFOA has been drawing increasing worldwide attention for treatment. Recent studies targeting on PFOA removal used different treatment such as ultrasonic treatment (Lin et al., 2016), sonochemical degradation with periodate (Lee et al., 2016), and microwave enhanced oxidation and reduction (Li et al., 2017), but they all involve complex operation and high energy cost. Significantly, heterogeneous photocatalysis is attractive due to the low energy consumption and high photocatalytic ability for PFOA degradation (Chen et al., 2015; Xu et al., 2018). A variety of materials used as the

catalysts also provide the possibility for the enhancement of this technology. Notably, Ga_2O_3, an environmentally friendly material, was found to be superior to TiO_2 when treating PFOA in solution (da Silva et al., 2017), and has several advantages such as chemical and biological stability, easy availability and nontoxicity. These characteristics enable it to be a frequently used catalyst in both research and industry applications (Lukic et al., 2017).

Furthermore, peroxymonosulfate (PMS, commercial name of Oxone®, $2KHSO_5 \cdot KHSO_4 \cdot K_2SO_4$) is an environmentally friendly oxidant (Khan et al., 2017). It can be activated by UV light to produce sulfate radicals ($SO_4^{\bullet -}$) which have strong oxidizing ability (Gao et al., 2016). A recent study (Wu et al., 2018) used persulfate-assisted photocatalytic ozonation, and their results revealed 99.2% removal of PFOA. Nevertheless, such significant research is limited, and still there is a research gap in the kinetics and mechanistic study of PFOA degradation in complex systems. This study aimed to investigate the photocatalytic ability of Ga_2O_3 assisted with PMS under UV light irradiation firstly used as the catalysts for PFOA photodegradation in water and wastewater. Experimental conditions such as catalyst amount and solution pH were evaluated by comparative experiments to explore the optimum conditions. Besides, the intermediates generated during the process and active species in charge of PFOA degrading were analysed to derive the possible photocatalytic mechanism in PMS/Ga_2O_3/UV system.

2. Materials and methods

2.1. Chemicals and materials

PFOA ($C_7F_{15}COOH$, 95%), perfluoroheptanoic acid (PFHpA, $C_6F_{13}COOH$, 99%), perfluorohexanoic acid (PFHxA, $C_5F_{11}COOH$, ≥ 97%), perfluoropentanoic acid (PFPeA, C_4F_9COOH, 97%), perfluorobutanoic acid (PFBA, C_3F_7COOH, 98%), pentafluoropropionic acid (PFPA, C_2F_5COOH, 97%) and trifluoroacetic acid (TFA, CF_3COOH, ≥ 99%) were

obtained from Sigma-Aldrich, Australia. Catalyst materials of gallium oxide (Ga_2O_3) and Oxone® were directly used without further treatment. The scavengers *tert*-butanol (*t*-BuOH), disodium ethylenediaminetetraacetate (EDTA-Na_2) and benzoquinone (BQ) were also obtained from Sigma-Aldrich. All solutions were prepared using ultra-pure water, obtained from distil chamber and a Milli-Q system.

2.2. UV irradiation experiments

A cylindrical reactor vessel was filled with PFOA aqueous solution of 200 mL and different initial PFOA concentrations (50 ng L^{-1}, 50 µg L^{-1}, 50 mg L^{-1}) at room temperature. The concentration of 50 mg L^{-1} was comparatively high, compared with the concentrations of PFOA occurring in the most contaminated water; it was also used as the initial concentration in a previous study (Chen et al., 2015). The solid catalyst of Ga_2O_3 was dispersed in PFOA solution, to which PMS was then added to initiate the reaction with continuous stirring for 30 min under darkness. The effect of solution pH on PFOA photodegradation was assessed by repeating experiments at pH 3, 5, 7 and 10. Light irradiation was provided by three separate lamps: a 32-W low-pressure UV lamp at 254 nm wavelength (Cnlight Co. Ltd., Shanghai, China), a 32-W low-pressure UV lamp at 185 nm wavelength (Cnlight Co. Ltd., Shanghai, China), and a 50-W xenon lamp at 400-800 nm wavelength (Nbet Co. Ltd., Beijing, China). The irradiation intensity of UV light (254 nm) was 1.71 mW cm^{-2} as measured by an UV intensity meter (ST-512). During photodegradation, the lamps were placed 5 cm above the liquid surface of the reactor and the solution was well mixed by magnetic stirring (Li et al., 2016; Zhao et al., 2015). At regular time intervals, aliquots of the sample were taken using a syringe and filtered through a filter (Puradisc syringe filter, 0.2 µm, Whatman) before analysis. For comparison, control experiments by Ga_2O_3, or PMS, or Ga_2O_3/PMS in darkness were conducted. In addition, photodegradation experiments by Ga_2O_3 or PMS under UV were

conducted. All experiments were conducted in triplicate. **Fig. A1** represents the overall process of the experiments.

2.3. Analytical methods

The characterization method for the catalysts were provided in the appendix. A triple quadrupole ultra-high-performance liquid chromatograph tandem mass spectrometer (UHPLC-MS/MS) from Shimadzu (model 8060) equipped with a binary pump and a Shim-pack column (1.6 μm, 2.0 mm × 50 mm) was used for the quantitative analysis of PFOA and its degradation products (PFHpA, PFHxA, PFPeA, PFBA, PFPrA, TFA). The mobile phase A was Milli-Q water and mobile phase B was methanol. The flow rate was 0.4 mL min^{-1} and the injection volume was 1 μL. The elution gradient of PFOA analysis method was initiated with 50% B for 2.5 min, then 100% B for the next 1 min followed by 50% B for another 1.5 min. The total run time of this method was 5 min. The mass spectrometer was operated in multiple reaction monitoring (MRM) mode. For PFOA, *m/z* 169.1 and *m/z* 219.0 are used as the qualitative ions and *m/z* 369.0 is used as the quantitation ion to avoid mass interference. The tandem mass spectrometry operating conditions of the target compounds are listed in **Table A1**.

3. Results and discussion

3.1. Photocatalytic ability of Ga_2O_3/PMS

The powder X-ray diffraction (XRD) pattern of Ga_2O_3 used in the study is shown in **Fig. A2**, which indicates that all of the diffraction peaks are in agreement with those of monoclinic phase of beta-Ga_2O_3 (JCPDS No. 41–1103) and the sharp diffraction peaks reveal that the samples has a high crystalline quality (Wang et al., 2015). The morphologies of these commercial catalysts were investigated by scanning electron microscope (SEM) and Ga_2O_3 shows to be rods with clear boundaries in **Fig. A3**.

In order to improve the catalytic efficacy, Ga_2O_3 was mixed with PMS in the PFOA solution as the catalysts for the PFOA degradation under UV light (254 nm). For strict comparison, the initial concentration of Ga_2O_3 was 0.25 g L^{-1} and PMS was 0.41 g L^{-1} so the molar ratio between Ga_2O_3 and PMS was 1:1. **Fig. 1A** shows that PFOA was completely degraded within 120 min by the catalysts of Ga_2O_3 mixed with PMS. However, when only PMS or Ga_2O_3 was used as the control group under the same condition, only 18% and 58.3% of PFOA was degraded, respectively within 180 min. Thus, the photocatalytic ability decreased as Ga_2O_3/PMS > Ga_2O_3 > PMS. The kinetics of the photodegradation of PFOA fitted well to the pseudo-first-order model ($R^2 > 0.90$) described by eq. 1:

$$\ln(C_0/C_t) = k\,t \qquad (1)$$

where k is the rate constant (min^{-1}), C_0 and C_t are the concentrations of PFOA (mg L^{-1}) in solution at irradiation time 0 and t, respectively. Based on the results in **Fig. 1A**, the rate constant for PFOA degradation according to system configuration or the type of catalyst used in the reactor (single or mixed catalyst) was found to be 0.0041 min^{-1}, 0.0013 min^{-1} and 0.0156 min^{-1}, for Ga_2O_3, PMS and Ga_2O_3/PMS, respectively. A catalyst combination of PMS/Ga_2O_3 significantly promoted the photocatalytic ability, resulting in 3.8 and 12 times higher rate constant than that of single Ga_2O_3 and PMS, respectively. Therefore, the results imply that sulfate radicals ($SO_4^{\bullet-}$) generated by PMS significantly enhanced the catalytic ability of Ga_2O_3 targeting on the PFOA degradation under UV irradiation. As the PMS/Ga_2O_3 system for PFOA photodegradation has not been studied before, their photocatalytic kinetics and mechanism were further investigated.

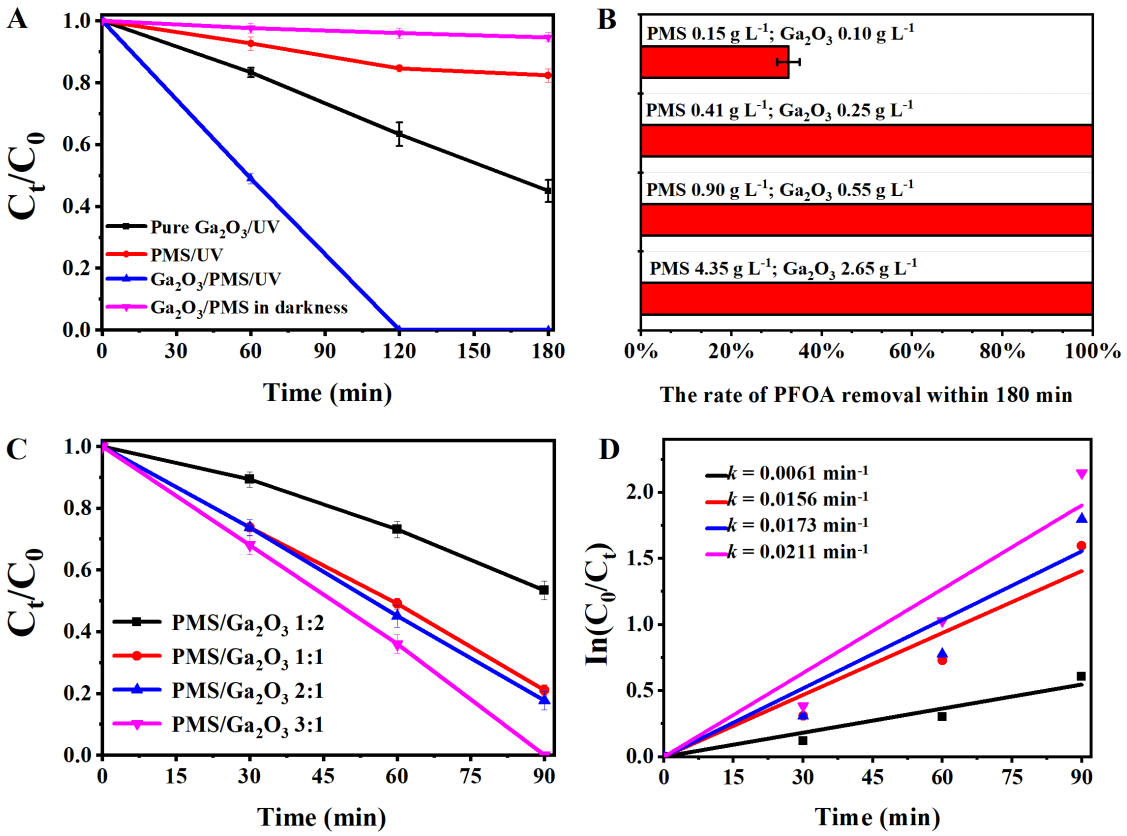

Fig. 1. Comparison of photocatalytic performance for PFOA removal among Ga_2O_3, PMS and Ga_2O_3/PMS under UV 254-nm (A). Degradation rate of PFOA by different amounts of PMS (0.16, 0.41, 0.90, 4.35 g L^{-1}) and Ga_2O_3 (0.10, 0.25, 0.55, 2.65 g L^{-1}) (B). Photocatalytic performance by different PMS/Ga_2O_3 ratios (1:2, 1:1, 2:1, 3:1) under UV 254-nm (C) and the fitting of degradation curves and rate constant (k) derived (D).

3.2. Factors influencing photodegradation efficiency

3.2.1. Effect of catalyst loading

Many previous studies have shown that the amount of catalyst has a positive effect on photocatalytic efficacy (Carbajo et al., 2018; Xu et al., 2017). Because the number of reactive sites increase with the increase of the catalyst amount that promote the rate of oxidation. However, a high concentration of catalyst would make the solution turbid, and reduce the photo permeability of UV light, with a negative effect on the photocatalytic degradation rate. In this study, under the 1:1 molar ratio of PMS and Ga_2O_3, different amounts of PMS/Ga_2O_3 (PMS at

4.35, 0.90, 0.41 and 0.16 g L^{-1}, Ga_2O_3 at 2.65, 0.55, 0.25 and 0.10 g L^{-1}) were used to assess the performance in PFOA removal. **Fig. 1B** shows that PMS ranging from 0.41 to 4.35 g L^{-1} and Ga_2O_3 ranging from 0.25 to 2.65 g L^{-1} generated identical results that 100% PFOA was degraded within 180 min. However, when the amount of PMS and Ga_2O_3 was decreased to 0.16 and 0.10 g L^{-1}, respectively, the degradation process was significantly inhibited, as only about 33% PFOA was removed during 180 min. This may be attributed to the reason that insufficient active groups produced in the system with a low concentration of Ga_2O_3 and PMS, which was also mentioned in the study by Carbajo et al. (2018). Compared with the previous study, 0.5 g L^{-1} TiO_2 doped with Pb could degrade almost 100% PFOA (50 mg L^{-1}) within 480 min at rate constant of 0.0086 min^{-1} (Chen et al., 2016), which was lower than that of Ga_2O_3/PMS (0.41 and 0.25 g L^{-1}) with the rate constant of 0.0156 min^{-1} in this study. Following the principle of low cost and high efficacy, the dosage of 0.41 g L^{-1} of PMS and 0.25 g L^{-1} of Ga_2O_3 were preferable under 1:1 molar ratio between PMS and Ga_2O_3 to obtain the most effective photodegradation.

Fig. 1C depicts the photocatalytic degradation process of aqueous PFOA in the presence of PMS/Ga_2O_3 with different PMS/Ga_2O_3 molar ratios such as 1:2, 1:1, 2:1 and 3:1 within 90 min. The dose of Ga_2O_3 was kept constant at 0.25 g L^{-1} while the amount of PMS was varied at 0.21, 0.41, 0.82, and 1.23 g L^{-1}. When the ratio was 3:1, the results showed that 100% PFOA was removed within 90 min. While lower ratio of PMS and Ga_2O_3 (i.e. 2:1, 1:1 and 1:2) resulted in lower PFOA degradation (i.e. 82%, 79% and 47%). Furthermore, the pseudo-first-order kinetics were used to evaluate the degradation of PFOA with different ratio of persulfate addition as shown in **Fig. 1D**. The rate constant increased with the increasing ratio of PMS/Ga_2O_3 in the system as $k_{3:1}$ = 0.0211 min^{-1} > $k_{2:1}$ = 0.0173 min^{-1} > $k_{1:1}$ = 0.0156 min^{-1} > $k_{1:2}$ = 0.0061 min^{-1}. The findings therefore suggest that $SO_4^{\bullet-}$ played a critical role in PMS/Ga_2O_3/UV system for PFOA degradation and a sufficient dose of PMS could boost the

degradation efficacy during the photocatalytic process. Thus, increasing the molar ratio between PMS and Ga_2O_3 from 1:2 to 3:1 would be better than increasing their individual amounts for PFOA removal.

3.2.2. Effect of solution pH

The photodegradation of PFOA was evaluated at various initial solution pH (pH 3, 5, 7 and 10) as shown in **Fig. 2A**. Under UV irradiation for 120 min, PFOA exhibited almost 100% removal at pH 3 which was decreased to 86% and 78% when pH was increased to 5 and 7, respectively. The removal of PFOA further dropped significantly to 27% under the basic condition of pH 10. Moreover, the degradation results followed the pseudo-first-order kinetic profile during the photocatalytic process under UV irradiation, with the rate constant decreasing as $k_{pH3} = 0.0156$ min^{-1} > $k_{pH5} = 0.0099$ min^{-1} > $k_{pH7} = 0.0084$ min^{-1} > $k_{pH10} = 0.0025$ min^{-1} (**Fig. 2B**). Hence, the degradation efficiency increased with lower solution pH. This could be attributed to the reaction between sulfate radicals ($SO_4^{\bullet-}$) and OH^- ions to form hydroxyl radicals (•OH) as shown in eq. 2 (Liang et al., 2007):

$$SO_4^{\bullet-} + OH^- \rightarrow SO_4^{2-} + \bullet OH \quad (2)$$

As previously reported, the hydroxyl radicals have poorer reactivity with PFOA in aqueous solution compared with $SO_4^{\bullet-}$ or photogenerated hole and electron pairs (Hori et al., 2004); thus, hydroxyl radicals production in the reaction system could slow down the PFOA degradation. Such a conclusion was also drawn from the research by Lee et al. (2009). In addition, in basic solution, abundant OH^- ions would react with •OH, which further inhibited the reaction of PFOA degradation following eq. 3:

$$\bullet OH + OH^- \rightarrow O^{\bullet-} + H_2O \quad (3)$$

On the other hand, the pH also affects the dissociation of ionizable chemicals such as PFOA in solution and consequently, influences their photocatalytic performance. As the pK_a is about 2.8 (Burns et al., 2008), PFOA in the aqueous solution is mainly in the protonated form

232 ($C_7F_{15}COOH$) at pH < 2.8 and the anionic form ($C_7F_{15}COO^-$) at pH > 2.8 based on eqs 4 and

233 5:

234 $$C_7F_{15}COOH = H^+ + C_7F_{15}COO^- \quad (4)$$

235 $$pKa = pH - \log\frac{C_7H_{15}{}^-}{C_7H_{15}COOH} \quad (5)$$

236 The zeta potential of Ga_2O_3 continuously decreased with the increased solution pH and the

237 points of zero charge (pH_{pzc}) was 8.6 as measured (**Fig. A4**), which is in accordance with the

238 research by Zhao et al. (2015). This suggests that when the solution pH was lower than 8.6, the

239 surface of Ga_2O_3 was positively charged due to the protonation; while over pH 8.6, the surface

240 of Ga_2O_3 was negatively charged. In addition, compounds adsorption on catalyst is a significant

241 step during the photocatalytic process. The lower the pH value is, the more positive the Ga_2O_3

242 surface will be. Therefore, comparatively high amount of PFOA was adsorbed on the surface

243 of Ga_2O_3 at pH 3 due to the Colombian attraction, promoting the photodegradation efficacy.

244 Zhao et al. (2015) proposed a similar explanation in their study.

245

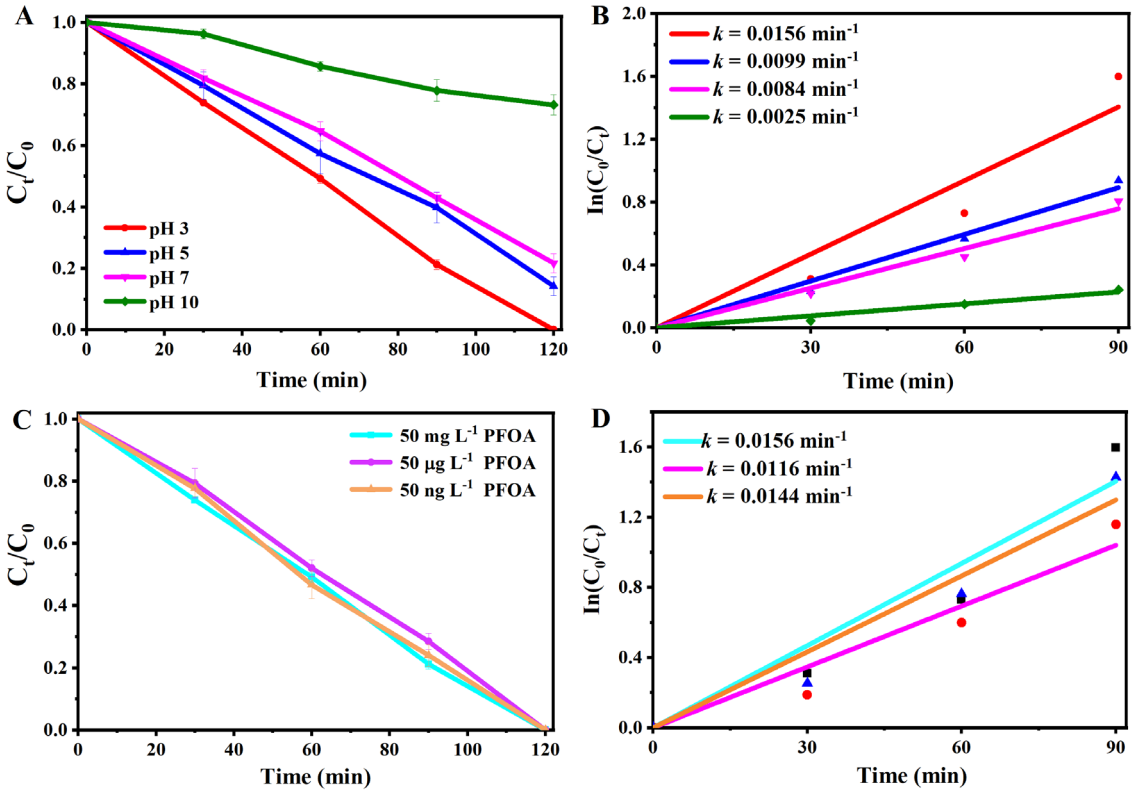

246

Fig. 2. Photocatalytic performance under different initial pH conditions (i.e. pH 3, pH 5, pH 7 and pH 10) activated in PMS/Ga_2O_3/UV system within 120 min ([PFOA] = 50 mg L^{-1}, [PMS] = 0.41 g L^{-1}, [Ga_2O_3] = 0.25 g L^{-1}) (A) and the fitting of degradation curves within 90 min and the rate constant (*k*) derived (B). Photocatalytic performance with initial PFOA concentration of 50 mg L^{-1}, 50 µg L^{-1} and 50 ng L^{-1} in PMS/Ga_2O_3/UV system within 120 min ([PMS] = 0.41 g L^{-1}, [Ga_2O_3] = 0.25 g L^{-1}) (C) and the fitting of degradation curves within 90 min and the rate constant (*k*) derived (D).

3.2.3. Effect of initial PFOA concentration

Initial PFOA concentration might affect the degradation rate (Hamid and Li, 2018; Tian and Gu, 2018). This study investigated three initial PFOA concentrations: 50 mg L^{-1}, 50 µg L^{-1} and 50 ng L^{-1}, to cover its likely levels in the aquatic environment. In the solution, PMS and Ga_2O_3 were set at 0.41 g L^{-1} and 0.25 g L^{-1}, respectively and the solution pH was adjusted to 3 to achieve the best performance of PFOA degradation. **Fig. 2C** shows that all three levels of concentration have similar degradation efficacy with similar rate constant at 0.0144–0.0156 min^{-1} (**Fig. 2D**), demonstrating that the photodegradation performance was relatively independent of initial PFOA concentrations. The results are due to the fact that 0.41 g L^{-1} of PMS and 0.25 g L^{-1} of Ga_2O_3 provided sufficient active sites and radicals, which completely degraded PFOA ranging from 50 ng L^{-1} to 50 mg L^{-1} at the similar degradation rate. Therefore, PMS/Ga_2O_3/UV system provided very effective treatment of PFOA whether at trace level (ng L^{-1}) or high level (mg L^{-1}), with great potential for decontaminating water and wastewater with varying degrees of pollution.

3.2.4. Effect of light sources

To explore the effect of light sources on the efficacy, photodegradation of PFOA (50 mg L^{-1}) under the optimum conditions (1.23 g L^{-1} PMS, 0.25 g L^{-1} Ga_2O_3, pH 3) were conducted

with both UV light (185 nm and 254 nm) and visible light (400–800 nm). **Fig. 3** presents that Ga_2O_3 with PMS under 185 nm UV light has higher degradation efficacy, as 100% PFOA was removed within 60 min. While under 254 nm UV light, the time spent for complete removal increased to 120 min. Furthermore, under visible light (400-800 nm), PFOA could only be degraded to a smaller extent. The results show that PMS/Ga_2O_3 absorption of 185 nm UV light was higher than that of 254 nm UV light, which in turn was significantly higher than that of visible light.

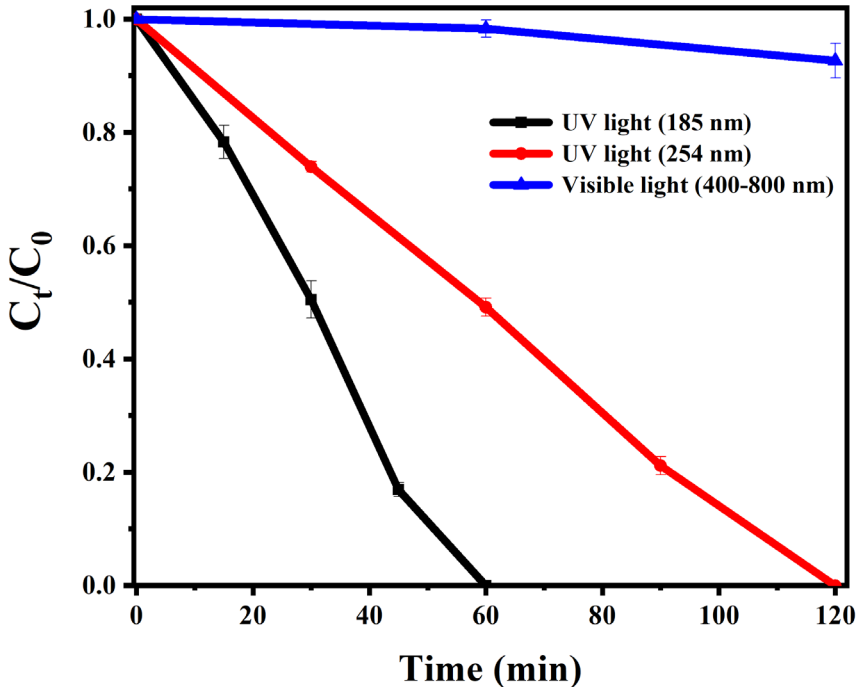

Fig. 3. Photocatalytic performance by PMS/Ga_2O_3 under UV light (185 nm, 254 nm) and visible light (400-800 nm) ([PMS] = 1.23 g L^{-1}, [Ga_2O_3] = 0.25 g L^{-1}).

Notably, Li et al. (2012; 2013a; 2013b) synthesized nanostructured In_2O_3 such as nanocubes, nanoplates and porous microsphere. Until now, these synthesized catalysts showed better performance of PFOA degradation under UV light (15 W, 254 nm) compared with other synthesized catalysts (i.e. Cu-TiO_2, TiO_2 nanotube arrays, Pb-$BiFeO_3$/RGO) in previous

studies (Chen et al., 2015; Shang et al., 2018; Wu et al., 2016), which could remove all PFOA (30 mg L^{-1}) within 30, 60 and 120 min, respectively. However, such catalysts need many precursors and solvothermal process for their synthesis, hence involving high cost. In this study, PMS/Ga_2O_3/UV system prepared by mixing the commercial Oxone and Ga_2O_3 at certain molar ratio (e.g. 3:1) under UV irradiation (32 W, 254 nm, 1.71 mW cm^{-2}) achieved comparatively high efficacy with complete removal of 50 mg L^{-1} PFOA in 90 min. Moreover, when the wavelength of UV light was changed to 185 nm, the degradation time was shortened to 60 min by PMS/Ga_2O_3. Therefore, PMS/Ga_2O_3/UV system has the advantages of being easily prepared, low cost and high degradation efficiency, hence demonstrating significant potential to be applied for PFAS removal in the aquatic environment.

3.3. Calculation of quantum yield

The results were analysed in terms of not only the first-order kinetic model, but also the explicit effect of photon absorption. The quantum yield (Φ), defined as moles of PFOA degraded per Einstein of photons absorbed by certain amount of catalysts, was estimated by eq. 6:

$$\Phi = \frac{Total\ number\ (moles) of\ PFOA\ degraded}{Total\ number\ (moles)\ of\ photons\ absorbed\ in\ the\ system} \quad (6)$$

The photocatalytic rate constant of the PFOA, *k*, under UV light (254 nm) can be used for the calculation of the reaction quantum yield as shown in eq. 7:

$$\Phi = \frac{k_{\Delta}}{I_a} \quad (7)$$

where k_{Δ} = $d(C_0\text{-}C_t)/dt$ (0.43 mg L^{-1} min^{-1}), and I_a is the photon numbers absorbed by the catalysts, which can be calculated by eq. 8:

$$I_a = \frac{E_p \times \left(1-10^{-2\cdot(\alpha(\lambda)\cdot C)\cdot z}\right)}{z} \times \frac{A1-A0}{A1} \quad (8)$$

where E_p is the average photon intensity (1.71 mW cm^{-2}), C is the concentration of the catalyst solution (2.8 mM) and z is the mixed depth of the water column (1.3 cm). In addition, A is the amount of light absorbed by the catalyst at wavelength 254 nm, which was detected by the spectrophotometer. α(λ) is the light attenuation coefficient of the catalysts which is calculated as:

$$\alpha(\lambda) = \frac{A}{Cl} \quad (9)$$

where l is the distance that light travels through the solution (1 cm). Based on the data summarized in **Table A2**, the quantum yield by the catalysts of PMS/Ga_2O_3 (0.41 g L^{-1} and 0.25 g L^{-1}, respectively) under UV light (254 nm) was 0.009 mol $Einstein^{-1}$. The details of calculation are presented in the supplemental material.

3.4. Application in wastewater treatment

Wastewater samples were taken from the influent and effluent of a municipal sewage treatment plant in Sydney, Australia, to prepare 50 mg L^{-1} of PFOA solution. The characteristics of the influent and effluent samples are listed in **Table A3.** When the PFOA and catalysts was added, the pH was changed to 3.0±0.2 without pH adjustment. Hereupon, photodegradation of PFOA under the optimum conditions (1.23 g L^{-1} PMS, 0.25 g L^{-1} Ga_2O_3, pH 3) were conducted with both UV light (185 nm and 254 nm). As shown in **Fig. 4A,** under 254 nm UV irradiation, 100% PFOA in wastewater was degraded by Ga_2O_3/PMS within 120 min with the rate constant of 0.012 min^{-1}, which was similar to that obtained in pure water. Under 185 nm UV irradiation, 60-75% PFOA in wastewater was removal at 30 min, and totally degraded within 60 min, which was also equal to the efficacy during treatment in pure water. Such findings indicated that photocatalysis by Ga_2O_3/PMS under UV light irradiation (254 and 185 nm) was highly stable and not easily disturbed by other organic compounds in the real wastewater. Besides, total organic carbon (TOC) was also analyzed before and after the treatment. As shown in **Fig. 4B**, in the effluent sample, 75% TOC was removed under 254 UV

light whereas 32% TOC was removed under 185 nm UV light. Similarly, in the influent sample, 85% TOC removal was observed under 254 nm UV, which was higher than 54% TOC removal under 185 nm UV. Thus, TOC could be significantly removed after the treatment under 254 nm UV light, which was better than that under 185 nm UV light. The reason might be related to fact that 185 nm UV does not transmit as well through water as does 254 nm UV (Imoberdorf et al, 2011). 254 nm UV light is fairly well transmitted as water molecules do not absorb the energy corresponding to this wavelength, while 185 nm intensity drops because it is absorbed by water molecules. Thus, 185 nm UV light is more powerful than 254 nm but poor transmitted in water, leading to the different degradation removal of TOC and PFOA in water and wastewater.

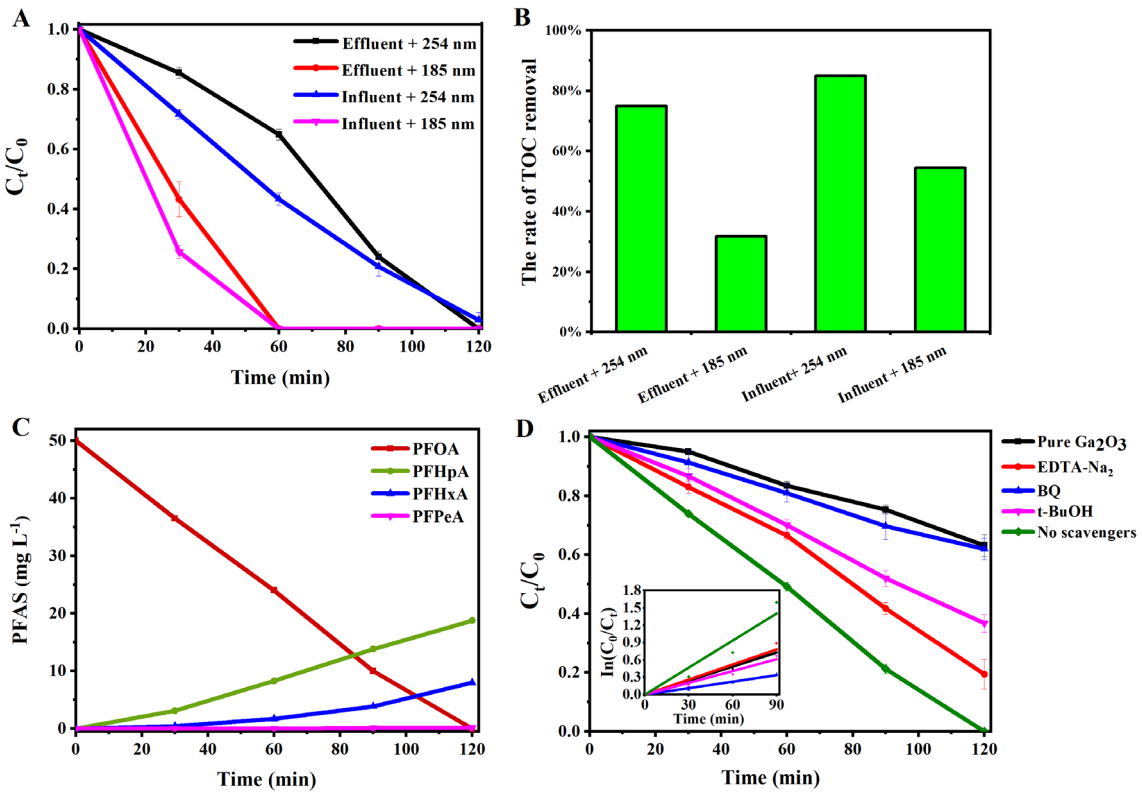

Fig. 4. Degradation of PFOA in wastewater samples including influent and effluent from a wastewater treatment plant under UV 254 nm and 185 nm (A). The rate of TOC removal by Ga_2O_3/PMS under 254 nm and 185 nm UV light. ([PFOA] = 50 mg L^{-1}, [PMS] = 0.45 g L^{-1},

350 [Ga_2O_3] = 0.25 g L^{-1}) (B). Evolution of PFOA and shorter-chain intermediates during PFOA
351 degradation in PMS/Ga_2O_3/UV system within 120 min (C). Effects of different scavengers (i.e.
352 Pure Ga_2O_3, EDTA-Na_2, BQ, *t*-BuOH, no scavengers) on the PFOA degradation in
353 PMS/Ga_2O_3/UV system within 120 min. Insert showing the fitting of degradation curves within
354 90 min and degradation rate constant (*k*) derived (D).
355
356 *3.5. Photocatalysis mechanism*
357 *3.5.1. Intermediates analysis*
358 Intermediates during PFOA photocatalytic process were identified and quantified with
359 UHPLC-MS/MS, which were the shorter-chain PFAS including PFHpA, PFHxA, PFPeA,
360 PFBA, PFPA and TFA as shown in **Fig. A5**. **Fig. 4C** presents the time-dependence of the
361 intermediates during the photodegradation process over PMS/Ga_2O_3 under 254 nm UV light
362 irradiation. PFHpA increased slowly to about 18.77 mg L^{-1} within 120 min, with the target
363 pollutant PFOA decreasing from 50 mg L^{-1} to nearly zero. The amount of PFHxA was
364 gradually increased to 7.98 mg L^{-1} within 120 min and PFPeA was firstly detected at 90 min
365 and slightly increased to 0.175 mg L^{-1} at 120 min. While species with shorter chains (i.e. PFBA
366 PFPA and TFA) had the low concentrations (below limit of quantification). This phenomenon
367 suggests that PFOA was degraded stepwise into shorter chain intermediates such as PFHpA,
368 PFHxA and PFPeA, which was consistent with the study by Lee et al. (2009).
369

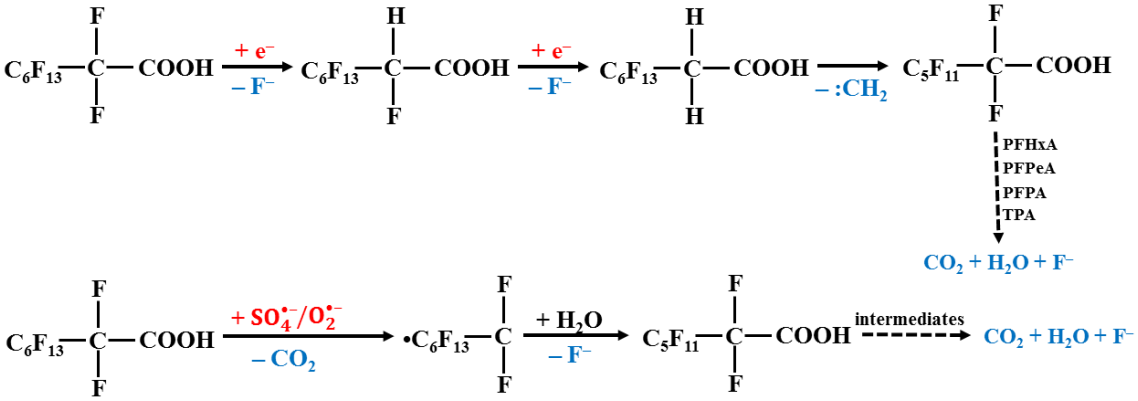

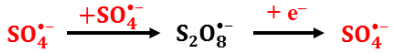

Fig. 5. The mechanism of PFOA degradation during the photocatalytic process in PMS/Ga_2O_3/UV system. The active species are marked in red, and the ion or compounds removed during degradation are marked in blue.

3.5.2. Analysis of active species

In PMS/Ga_2O_3/UV system, five types of active species including sulfate radicals ($SO_4^{\bullet-}$), photoinduced holes (h^+) and electrons (e^-), hydroxyl radicals (•OH), and superoxide radical anions ($O_2^{\bullet-}$), could be produced during the photocatalytic process as shown in eqs 10-13 (Chen et al., 2016):

$$HSO_5^- + hv \rightarrow SO_4^{\bullet-} + \bullet OH \quad (10)$$

$$Ga_2O_3 + hv \rightarrow Ga_2O_3\ (h^+ + e^-) \quad (11)$$

$$h^+ + H_2O \rightarrow \bullet OH + H^+ \quad (12)$$

$$e^- + O_2 \rightarrow O_2^{\bullet-} \quad (13)$$

To confirm which active species take the leading place in the photocatalytic reaction, *t*-BuOH, EDTA-Na_2 and BQ were added to the system, which were used as scavengers of •OH, holes and $O_2^{\bullet-}$, respectively. Besides, degradation by Ga_2O_3 only was used to simulate the condition of adding the scavenger of $SO_4^{\bullet-}$ radicals. **Fig. 4D** shows these scavengers effect on the

photocatalysis in PMS/Ga_2O_3/UV system and the rate constants were provided during 90 min of the photocatalytic process. When no scavengers were added, 100% PFOA could be degraded within 120 min with the rate constant of 0.156 min^{-1}. However, during the degradation by Ga_2O_3 only (equivalent to the scavenging of $SO_4^{\bullet-}$), the degradation rate dropped to 47%, and the rate constant decreased to 0.0081 min^{-1}. The results suggested that $SO_4^{\bullet-}$ produced by PMS was a critically important oxidant for PFOA degradation in the photocatalytic system. Similarly, when BQ was added in the PFOA solution, the degradation rate was significantly reduced to 38% and the rate constant was 0.0037 min^{-1}, indicating that $O_2^{\bullet-}$ radicals generated by electrons also had high oxidative power for PFOA degradation. In addition, *t*-BuOH added in the solution resulted in 63% PFOA removal with the rate constant of 0.0068 min^{-1}. The findings indicated that •OH radicals should be a secondary active species compared with $SO_4^{\bullet-}$ and $O_2^{\bullet-}$ radicals reacting with PFOA under UV irradiation. Additionally, when EDTA-Na_2 was added in the system, only a slight decrease was observed on the degradation rate compared with that of no scavenger addition, as 80% PFOA was degraded within 120 min and the rate constant could reach 0.0087 min^{-1}. Such findings suggested that photogenerated electrons rather than photogenerated holes were the main factor promoting the photocatalytic efficacy, which are consistent with the study conducted by Zhao et al. (2015). Conclusively, the results proved that the $SO_4^{\bullet-}$ radicals produced by PMS, $O_2^{\bullet-}$ radicals, and photogenerated electrons (e^-) played major roles in degrading PFOA in the PMS/Ga_2O_3/UV system. The •OH radicals are of secondary importance while photogenerated holes have little effect on the degradation efficacy.

3.5.3. Photocatalytic process

According to the intermediates presence and main active species photogenerated electrons (e^-), $SO_4^{\bullet-}$ and $O_2^{\bullet-}$ radicals during the photocatalytic process as mentioned above, the PFOA degradation process can be described as follows. First, the fluorine atom was more

preferable than the carbon atom to react with photo-induced electron (e^-), leading to the cleavage of C-F bonds, similar to previous study on perfluorocarboxylates photodegradation (Qu et al., 2010; Song et al., 2013). Moreover, the α-position C-F bond was more easily attacked by e^- due to the inductive effect of the carboxyl in PFOA. Thus, fluorine was eliminated from PFOA to form $C_7F_{13}H_2COOH$:

$$C_7F_{15}COOH + e^- \rightarrow \bullet C_7F_{14}COOH + F^- \quad (14)$$

$$\bullet C_7F_{14}COOH + H_2O \rightarrow C_7F_{14}HCOOH + \bullet OH \quad (15)$$

$$C_7F_{14}HCOOH + e^- \rightarrow \bullet C_7F_{13}COOH + F^- \quad (16)$$

$$\bullet C_7F_{13}COOH + H_2O \rightarrow C_7F_{13}H_2COOH + \bullet OH \quad (17)$$

$C_7F_{13}H_2COOH$ was excited by UV irradiation to generate C_6F_{13} radical, COOH radical and CH_2 carbene. Then C_6F_{13} and COOH radical could recombine to form PFHpA ($C_6F_{13}COOH$):

$$C_7F_{13}H_2COOH \rightarrow \bullet C_6F_{13} + :CH_2 + \bullet COOH \quad (18)$$

$$\bullet C_6F_{13} + \bullet COOH \rightarrow C_6F_{13}COOH \text{ (PFHpA)} \quad (19)$$

Consequently, PFHpA was decomposed into PFHxA and PFPeA, and theoretically, it would continue degradation to form PFBA, PFPA and TPA in the same way and finally become mineralized to CO_2 and fluoride ions in the stepwise manner as reported by Li et al. (2013b).

In the Ga_2O_3/UV system, when the adsorption of photon energy is equal or more than the band gap energy of Ga_2O_3, holes and electrons are generated on the surface of Ga_2O_3 particles due to the irradiation of UV light. Notably, the photo-induced electrons were the main active species for PFOA degradation as mentioned in the previous section, which were also reported by Trojanowicz et al. (2018). However, the recombination of the photo-induced hole and electron could seriously reduce the photocatalytic efficiency (Li et al., 2018). In the PMS/Ga_2O_3/UV system, sulfate radical anions ($SO_4^{\bullet -}$) and $O_2^{\bullet -}$ can oxidize PFOA into perfluorinated alkyl radicals ($\bullet C_7F_{15}$):

$$SO_4^{\bullet -} + C_7F_{15}COOH \rightarrow SO_4^{2-} + \bullet C_7F_{15}COOH^+ \quad (20)$$

438 $$\bullet C_7F_{15}COOH^+ \rightarrow \bullet C_7F_{15} + CO_2 + H^+ \quad (21)$$

439 $$C_7F_{15}COOH + O_2^{\bullet -} \rightarrow \bullet C_7F_{15} + CO_2\uparrow \quad (22)$$

440 Then formed C_7F_{15} radical react with water to form $C_6F_{13}COF$ after H^+ and F^- elimination:

441 $$\bullet C_7F_{15} + H_2O \rightarrow C_7F_{15}OH + H^+ \quad (23)$$

442 $$C_7F_{15}OH \rightarrow C_6F_{13}COF + HF \quad (24)$$

443 By hydrolysis, $C_6F_{13}COF$ is converted into PFHpA ($C_6F_{13}COOH$) with CF_2 units reduced and
444 followed by a stepwise degradation of PFOA to form shorter chain PFAS:

445 $$C_6F_{13}COF + H_2O \rightarrow C_6F_{13}COOH\ (PFHpA) + HF \quad (25)$$

446 Furthermore, the excited e^- could activate MPS to produce $SO_4^{\bullet -}$ radicals, which have
447 been demonstrated in a previous study (Liu et al., 2017). These processes could explain that
448 photodegradation efficiency was much better in PMS/Ga_2O_3/UV system than by sole Ga_2O_3 or
449 PMS:

450 $$SO_4^{\bullet -} + SO_4^{\bullet -} \rightarrow S_2O_8^{2-} \quad (26)$$

451 $$S_2O_8^{2-} + e^- \rightarrow SO_4^{\bullet -} \quad (27)$$

452 Overall, the mechanism during the photocatalysis process of PFOA degradation in the
453 PMS/Ga_2O_3/UV system is postulated in **Fig. 5**.

454

455 **4. Conclusions**

456 PFOA removal from aqueous solution was studied by UV photocatalysis using Ga_2O_3
457 and further enhanced in the presence of PMS. Specifically, the application of 1.23 g L^{-1} of PMS
458 and 0.25 g L^{-1} of Ga_2O_3 was able to degrade 100% PFOA in aqueous solution within 90 min
459 under UV 254 nm and 60 min under UV 185 nm. Furthermore, acidic condition at pH 3 was
460 favourable for PFOA degradation in PMS/Ga_2O_3/UV system. Such degradation was not
461 affected by the initial concentration of PFOA ranged from 50 ng L^{-1} to 50 mg L^{-1}. The quantum
462 yield during photocatalysis by PMS/Ga_2O_3 under UV light (254 nm) was 0.009 mol Einstein$^-$

463 [1]. Through the analysis of intermediates, PFOA was gradually degraded from long chian
464 species into short chain intermediates. Scavenger experiments proved that $SO_4^{\bullet-}$ radicals, $O_2^{\bullet-}$
465 radicals and photogenerated electrons were the most important active species contributing to
466 the PFOA photodegradation. PFOA in real wastewater could be also treated by Ga_2O_3/PMS
467 under UV light irradiation with similar degradation performance to pure water, in addition to
468 75-85% TOC removal after the treatment by 254 nm UV light. Overall, the PMS/Ga_2O_3/UV
469 system has great potential to be applied in the photodegradation of PFOA and other similar
470 organic pollutants in water and wastewater.
471
472 **Acknowledgements**
473 The authors would like to thank the China Scholarship Council (CSC) for financial
474 support (Grant No. 201606890028).
475
476 **References**
477 Anderson, R.H., Adamson, D.T., Stroo, H.F., 2018. Partitioning of poly-and perfluoroalkyl
478 substances from soil to groundwater within aqueous film-forming foam source zones.
479 J. Contam. Hydrol. 220, 59-65.
480 Apelberg, B.J., Witter, F.R., Herbstman, J.B., Calafat, A.M., Halden, R.U., Needham, L.L.,
481 Goldman, L.R., 2007. Cord serum concentrations of perfluorooctane sulfonate (PFOS)
482 and perfluorooctanoate (PFOA) in relation to weight and size at birth. Health Perspect.
483 115, 1670-1676.
484 Blake, B.E., Pinney, S.M., Hines, E.P., Fenton, S.E., Ferguson, K.K., 2018. Associations
485 between longitudinal serum perfluoroalkyl substance (PFAS) levels and measures of
486 thyroid hormone, kidney function, and body mass index in the Fernald Community
487 Cohort. Environ. Pollut. 242, 894-904.

488 Braunig, J., Baduel, C., Barnes, C.M., Mueller, J.F., 2019. Leaching and bioavailability of
489 selected perfluoroalkyl acids (PFAAs) from soil contaminated by firefighting activities.
490 Sci. Total Environ. 646, 471-479.
491 Burns, D.C., Ellis, D.A., Li, H., McMurdo, C.J., Webster, E., 2008. Experimental pKa
492 determination for perfluorooctanoic acid (PFOA) and the potential impact of pKa
493 concentration dependence on laboratory-measured partitioning phenomena and
494 environmental modeling. Environ. Sci. Technol. 42, 9283-9288.
495 Carbajo, J., Tolosana-Moranchel, A., Casas, J., Faraldos, M., Bahamonde, A., 2018. Analysis
496 of photoefficiency in TiO_2 aqueous suspensions: Effect of titania hydrodynamic particle
497 size and catalyst loading on their optical properties, Appl. Catal. B 221, 1-8.
498 Chen, M.J., Lo, S.L., Lee, Y.C., Huang, C.C., 2015. Photocatalytic decomposition of
499 perfluorooctanoic acid by transition-metal modified titanium dioxide. J. Hazard. Mater.
500 288, 168-175.
501 Chen, M.J., Lo, S.L., Lee, Y.C., Kuo, J., Wu, C.H., 2016, Decomposition of perfluorooctanoic
502 acid by ultraviolet light irradiation with Pb-modified titanium dioxide. J. Hazard.
503 Mater. 303, 111-8.
504 da Silva, F.L., Laitinen, T., Pirilä, M., Keiski, R.L., Ojala, S., 2017. Photocatalytic Degradation
505 of Perfluorooctanoic Acid (PFOA) From Wastewaters by TiO_2, In_2O_3 and Ga_2O_3
506 Catalysts. Top. Catal. 60, 1345-1358.
507 Gao, H., Chen, J., Zhang, Y., Zhou, X., 2016. Sulfate radicals induced degradation of Triclosan
508 in thermally activated persulfate system. Chem. Eng. J. 306, 522-530.
509 Hamid, H., Li, L.Y., 2018. Fate of perfluorooctanoic acid (PFOA) in sewage sludge during
510 microwave-assisted persulfate oxidation treatment. Environ. Sci. Pollut. Res. 25,
511 10126-10134.

512 Holtcamp, W., 2012. Pregnancy-induced hypertension “probably linked” to PFOA
513 contamination. Environ. Health Perspect. 120, A55-A59.
514 Hori, H., Hayakawa, E., Einaga, H., Kutsuna, S., Koike, K., Ibusuki, T., Kiatagawa, H.,
515 Arakawa, R., 2004. Decomposition of environmentally persistent perfluorooctanoic
516 acid in water by photochemical approaches. Environ. Sci. Technol. 38, 6118-6124.
517 Imoberdorf, G., Mohseni, M., 2011. Degradation of natural organic matter in surface water
518 using vacuum-UV irradiation. J. Hazard. Mater. 186 (1), 240-246.
519 Janda, J., Nödler, K., Brauch, H.J., Zwiener, C., Lange, F.T., 2019. Robust trace analysis of
520 polar (C2-C8) perfluorinated carboxylic acids by liquid chromatography-tandem mass
521 spectrometry: method development and application to surface water, groundwater and
522 drinking water. Environ. Sci. Pollut. Res. 26, 7326-7336.
523 Jian, J.M., Chen, D., Han, F.J., Guo, Y., Zeng, L., Lu, X., Wang, F., 2018. A short review on
524 human exposure to and tissue distribution of per-and polyfluoroalkyl substances
525 (PFASs). Sci. Total Environ. 636, 1058-1069.
526 Khan, S., He, X., Khan, J.A., Khan, H.M., Boccelli, D.L., Dionysiou, D.D., 2017. Kinetics and
527 mechanism of sulfate radical- and hydroxyl radical-induced degradation of highly
528 chlorinated pesticide lindane in UV/peroxymonosulfate system. Chem. Eng. J. 318,
529 135-142.
530 Lee, Y.C., Chen, M.J., Huang, C.P., Kuo, J., Lo, S.L., 2016. Efficient sonochemical
531 degradation of perfluorooctanoic acid using periodate. Ultrason. Sonochem. 31, 499-
532 505.
533 Lee, Y.C., Lo, S.L., Chiueh, P.T., Chang, D.G., 2009. Efficient decomposition of
534 perfluorocarboxylic acids in aqueous solution using microwave-induced persulfate.
535 Water Res. 43, 2811-2816.

536 Li, D., Yu, J.C.C., Nguyen, V.H., Wu, J.C., Wang, X., 2018. A dual-function photocatalytic
537 system for simultaneous separating hydrogen from water splitting and photocatalytic
538 degradation of phenol in a twin-reactor. Appl. Catal. B 239, 268-279.
539 Li, M., Yu, Z., Liu, Q., Sun, L., Huang, W., 2016. Photocatalytic decomposition of
540 perfluorooctanoic acid by noble metallic nanoparticles modified TiO_2. Chem. Eng. J.
541 286, 232-238.
542 Li, S., Zhang, G., Zhang, W., Zheng, H., Zhu, W., Sun, N., Zheng, Y., Wang, P., 2017.
543 Microwave enhanced Fenton-like process for degradation of perfluorooctanoic acid
544 (PFOA) using Pb-$BiFeO_3$/rGO as heterogeneous catalyst. Chem. Eng. J. 326, 756-764.
545 Li, Z., Zhang, P., Li, J., Shao, T., Jin, L., 2013a., Synthesis of In_2O_3-graphene composites and
546 their photocatalytic performance towards perfluorooctanoic acid decomposition. J.
547 Photochem. Photobiol. A 271, 111-116.
548 Li, Z., Zhang, P., Shao, T., Li, X., 2012. In_2O_3 nanoporous nanosphere: A highly efficient
549 photocatalyst for decomposition of perfluorooctanoic acid. Appl. Catal. B 125, 350-
550 357.
551 Li, Z., Zhang, P., Shao, T., Wang, J., Jin, L., Li, X., 2013b. Different nanostructured In_2O_3 for
552 photocatalytic decomposition of perfluorooctanoic acid (PFOA). J. Hazard. Mater. 260,
553 40-46.
554 Liang, C., Wang, Z-S., Bruell, C.J., 2007. Influence of pH on persulfate oxidation of TCE at
555 ambient temperatures. Chemosphere 66, 106-113.
556 Lin, J.C., Hu, C.Y., Lo, S.L., 2016. Effect of surfactants on the degradation of
557 perfluorooctanoic acid (PFOA) by ultrasonic (US) treatment. Ultrason. Sonochem. 28,
558 130-135.

559 Liu, Y., Zhang, Y., Guo, H., Cheng, X., Liu, H., Tang, W., 2017. Persulfate-assisted
560 photodegradation of diethylstilbestrol using monoclinic $BiVO_4$ under visible-light
561 irradiation. Environ. Sci. Pollut. Res. 24, 3739-3747.
562 Lukic, S., Menze, J., Weide, P., Busser, G.W., Winterer, M., Muhler, M., 2017. Decoupling
563 the Effects of High Crystallinity and Surface Area on the Photocatalytic Overall Water
564 Splitting over β-Ga2O3 Nanoparticles by Chemical Vapor Synthesis. ChemSusChem
565 10, 4190-4197.
566 Mastrantonio, M., Bai, E., Uccelli, R., Cordiano, V., Screpanti, A., Crosignani, P., 2017.
567 Drinking water contamination from perfluoroalkyl substances (PFAS): an ecological
568 mortality study in the Veneto Region, Italy. European J. Public Health 28, 180-185.
569 Mazzoni, M., Buffo, A., Cappelli, F., Pascariello, S., Polesello, S., Valsecchi, S., Volta, P.,
570 Bettinetti, R., 2019. Perfluoroalkyl acids in fish of Italian deep lakes: Environmental
571 and human risk assessment. Sci. Total Environ. 653, 351-358.
572 Mulabagal, V., Liu, L., Qi, J., Wilson, C., Hayworth, J.S., 2018. A rapid UHPLC-MS/MS
573 method for simultaneous quantitation of 23 perfluoroalkyl substances (PFAS) in
574 estuarine water. Talanta 190, 95-102.
575 Qu, Y., Zhang, C., Li, F., Chen, J., Zhou, Q., 2010. Photo-reductive defluorination of
576 perfluorooctanoic acid in water. Water Res. 44, 2939-2947.
577 Saleh, N.B., Khalid, A., Tian, Y., Ayres, C., Sabaraya, I.V., Pietari, J., Hanigan, D.,
578 Chowdhury, I., Apul, O.G., 2019. Removal of poly-and per-fluoroalkyl substances
579 from aqueous systems by nano-enabled water treatment strategies. Environ. Sci. Water
580 Res. Technol. 5, 198-208.
581 Shang, E., Li, Y., Niu, J., Li, S., Zhang, G., Wang, X., 2018. Photocatalytic degradation of
582 perfluorooctanoic acid over Pb-BiFeO3/rGO catalyst: Kinetics and mechanism.
583 Chemosphere 211, 34-43.

584 Song, Z., Tang, H., Wang, N., Zhu, L., 2013. Reductive defluorination of perfluorooctanoic
585 acid by hydrated electrons in a sulfite-mediated UV photochemical system. J. Hazard.
586 Mater. 262, 332-338.
587 Tian, H., Gu, C., 2018. Effects of different factors on photodefluorination of perfluorinated
588 compounds by hydrated electrons in organo-montmorillonite system. Chemosphere
589 191, 280-287.
590 Trojanowicz, M., Bojanowska-Czajka, A., Bartosiewicz, I., Kulisa, K., 2018. Advanced
591 oxidation/reduction processes treatment for aqueous perfluorooctanoate (PFOA) and
592 perfluorooctanesulfonate (PFOS)–a review of recent advances. Chem. Eng. J. 336, 170-
593 199.
594 Wang, Y., Li, N., Duan, P., Sun, X., Chu, B., He, Q., 2015. Properties and photocatalytic
595 activity of β-Ga_2O_3 nanorods under simulated solar irradiation. J. Nanomater. 16, 126.
596 Wu, D., Li, X., Zhang, J., Chen, W., Lu, P., Tang, Y., Li, L., 2018. Efficient PFOA degradation
597 by persulfate-assisted photocatalytic ozonation. Sep. Purif. TechnoL. 207, 255-261.
598 Wu, Y., Li, Y., Tian, A., Mao, K., Liu, J., 2016. Selective removal of perfluorooctanoic acid
599 using molecularly imprinted polymer-modified TiO_2 nanotube arrays. Int. J.
600 Photoenergy 2016, 1-10.
601 Xu, B., Ahmed, M.B,. Zhou, J.L., Altaee, A., Wu, M., Xu, G., 2017. Photocatalytic removal of
602 perfluoroalkyl substances from water and wastewater: Mechanism, kinetics and
603 controlling factors. Chemosphere 189, 717-729.
604 Xu, B., Ahmed, M.B., Zhou, J.L., Altaee, A., Xu, G., Wu, M., 2018. Graphitic carbon nitride
605 based nanocomposites for the photocatalysis of organic contaminants under visible
606 irradiation: Progress, limitations and future directions. Sci. Total Environ. 633, 546-
607 559.

608 Zhao, B., Li, X., Yang, L., Wang, F., Li, J., Xia, W., Li, W., Zhou, L., Zhao, C., 2015. β-Ga_2O_3
609 nanorod synthesis with a one-step microwave irradiation hydrothermal method and its
610 efficient photocatalytic degradation for perfluorooctanoic acid. Photochem. Photobiol.
611 91, 42-47.